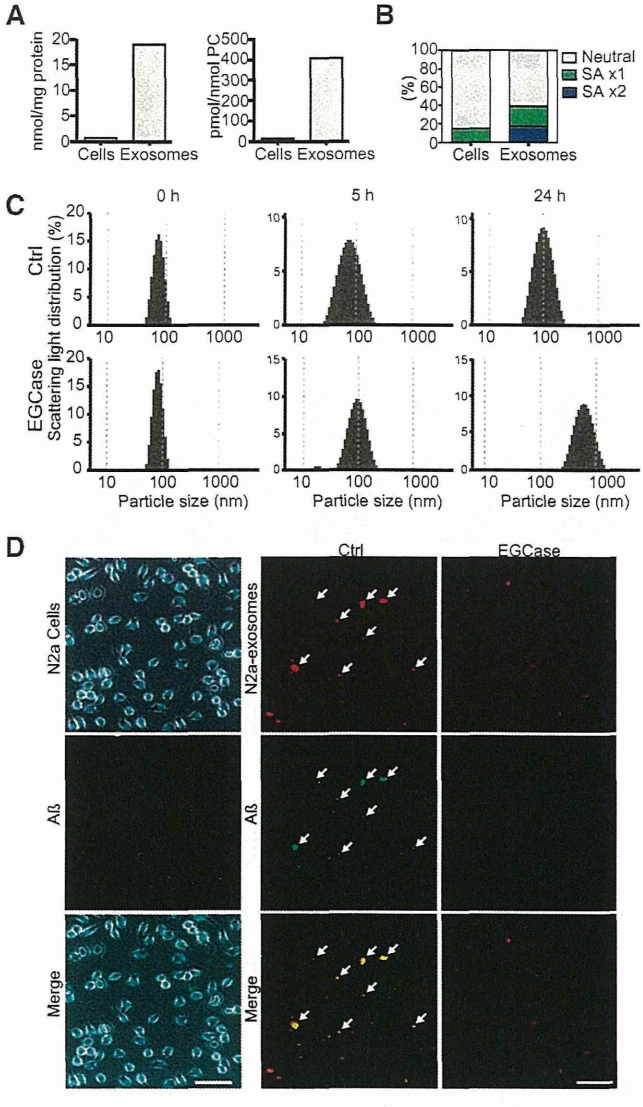

FIGURE 5. **Exosomal GSLs are responsible for Aβ binding on the vesicles.** Exosomal and cellular glycomes of GSLs were surveyed by mass spectrometry. *A*, total amounts of GSL-glycans in exosomes and their originating cells were determined by standardization with protein or phosphatidylcholine (*PC*) content. *B*, GSLs other than GM2 detected in exosomes or cells were classified according to the number of sialic acid moieties. *C*, particle size of exosomes (untreated or treated with EGCase) was determined by dynamic light scattering analysis after incubating them at 37 °C for 0, 5, and 24 h. *D*, representative images of Aβ binding on N2a cells and exosomes (untreated as Ctrl or treated with EGCase, *red*) after 5 h incubation with fluorescent $A\beta_{1-42}$ (1 μM, *green*). The cells were stained with DAPI. *Arrows* indicate Aβ fluorescence co-localized with exosomal signals. *Scale bar*, 25 μm (N2a cells) and 10 μm (exosomes) *E*, surface plasmon resonance sensorgrams showing the interactions of N2a-derived exosomes (1 μg of protein/μl) with immobilized $A\beta_{1-42}$ or $A\beta_{42-1}$. The responses were subtracted from a blank surface prepared by ethanolamine deactivation. *RU*, resonance units. *F*, sensorgrams showing the interactions of the exosomes (untreated (Ctrl) or pretreated with EGCase, 1 μg of protein/μl) with immobilized $A\beta_{1-40}$, $A\beta_{1-42}$, or $A\beta_{1-38}$. The resultant responses were subtracted from a surface that was immobilized with BSA.

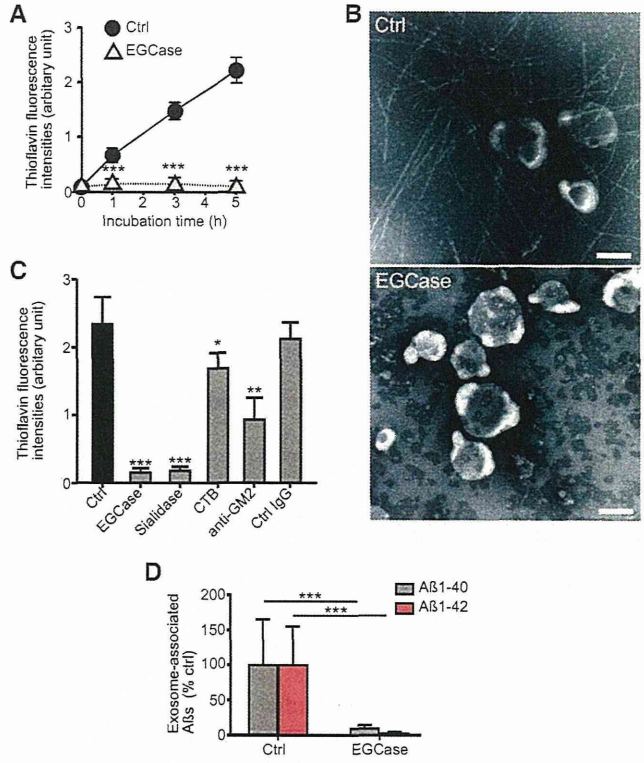

FIGURE 6. **Exosomal GSLs are involved in Aβ assembly.** *A*, thioflavin fluorescence intensities were measured in mixtures of exosomes (untreated as Ctrl or treated with EGCase) incubated with 15 μM $A\beta_{1-42}$. Data are presented as the mean ± S.D.; ***, $p < 0.001$ ($n = 4$). *B*, representative electron microscopic images of exosomes incubated for 5 h with 15 μM $A\beta_{1-42}$ are shown. *Scale bar*, 100 nm. *C*, the exosomes (untreated as Ctrl or treated with EGCase or sialidase) were incubated for 5 h with 15 μM $A\beta_{1-42}$. The untreated exosomes were reacted with Aβ in the presence of cholera toxin B subunit (*CTB*) or anti-GM2 antibody. Fluorescence intensities of thioflavin-T were then measured. Values in each column are the mean ± S.D. of five values. *, $p < 0.05$; **, $p < 0.01$; ***, $p < 0.001$. *D*, biotinylated exosomes (untreated as Ctrl or treated with EGCase) stereotaxically injected into the hippocampus of APP mice (4 months) were isolated at 3 h after the injection, and the levels of exosome-associated Aβ were quantified by ELISA. Values are the mean ± S.D., ***, $p < 0.001$ ($n = 4$).

microdomains to drive domain-induced budding of biological membranes (25), which results in highly loading Cer and its vicinal lipid molecules into the generated vesicle. Indeed, Cer and SM are concentrated in exosome membranes (Fig. 7) (23). In addition, SM forms a distinct membrane domain, namely a lipid raft, in the plasma membrane together with GSLs and cholesterol (26). Various raft-resident proteins have also been reported to be abundant in exosomes (27).

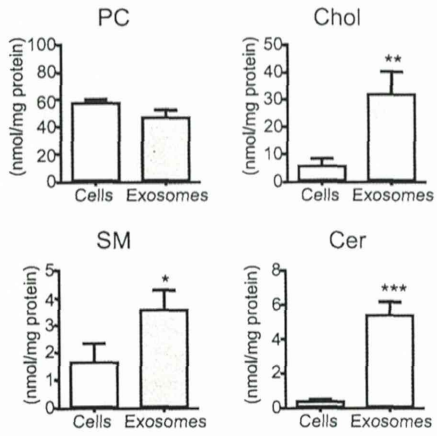

FIGURE 7. **Exosomal and cellular lipid analysis.** Levels of phosphatidylcholine (*PC*), cholesterol (*Chol*), sphingomyelin (*SM*), and ceramide (*Cer*) were measured in N2a cells and the isolated exosomes. The data presented are the mean ± S.D. from three independent experiments; *, $p < 0.05$; **, $p < 0.01$; ***, $p < 0.001$.

In the present study, providing GSLs-enriched exosomes to the APP mouse brains resulted in recovering synaptic impairment and decreasing Aβ plaques. However, the effect of GSLs on AD pathogenesis is a controversial issue. GSL storage disorders, which are subtypes of lysosomal storage diseases caused by genetic dysfunction in GSL catabolism, share pathological features with AD, such as Aβ burden (28, 29). Accumulated gangliosides are observed in human brains exhibiting AD, and they are proposed to contribute to AD development through promoting Aβ fibril formation (16). These discrepant effects of GSLs are likely to stem from their life span in brain tissues. Pathologically accumulated GSLs are pooled within cells to form complexes with Aβ and its polymer (19, 28), which might be retained to exert neuronal damages. On the other hand, exosomal GSLs capture Aβ in extracellular fluid and are rapidly taken up by phagocytes without persistent harm to the brain.

Our present study demonstrated that exosomes derived from N2a cells can promote Aβ fibril formation on their surface (Fig. 6, *A* and *B*). The exosome-bound Aβ was then incorporated into microglia for degradation (Figs. 1*E* and 8, *A* and *B*) (8). Therefore, continuous infusion of exosomes induced a reduction in amyloid depositions in aged APP mouse brains (Fig. 3*C*). These results provide a notion that the exosomes in the brains are rapidly cleared by microglia before the exosome-bound Aβs form amyloid fibrils for depositions. Amyloid plaques were reported to change their sizes over days in the brains of AD model mice (30). The exogenously added exosomes might prevent further Aβ depositions by blocking the supply of the soluble Aβ. Alternatively, exosomes might support the clearance of amyloid deposit, which already formed. The complex of GM1-Aβ has been reported to localize at the ends of extended Aβ fibrils in the incubation mixture of GM1 and Aβ (19). Alix, a marker for exosomes was enriched around the small Aβ plaques in brain sections from AD patients (6). Similarly, once the exogenous exosome-associated Aβs are attached to the Aβ fibrils in the amyloid plaques, they might provoke microglia gathering toward the plaques and accelerate their clearance.

Here, we used seed-free Aβ to perform the Aβ binding assay (Fig. 5*D*) and the surface plasmon resonance analysis (Fig. 5*E*

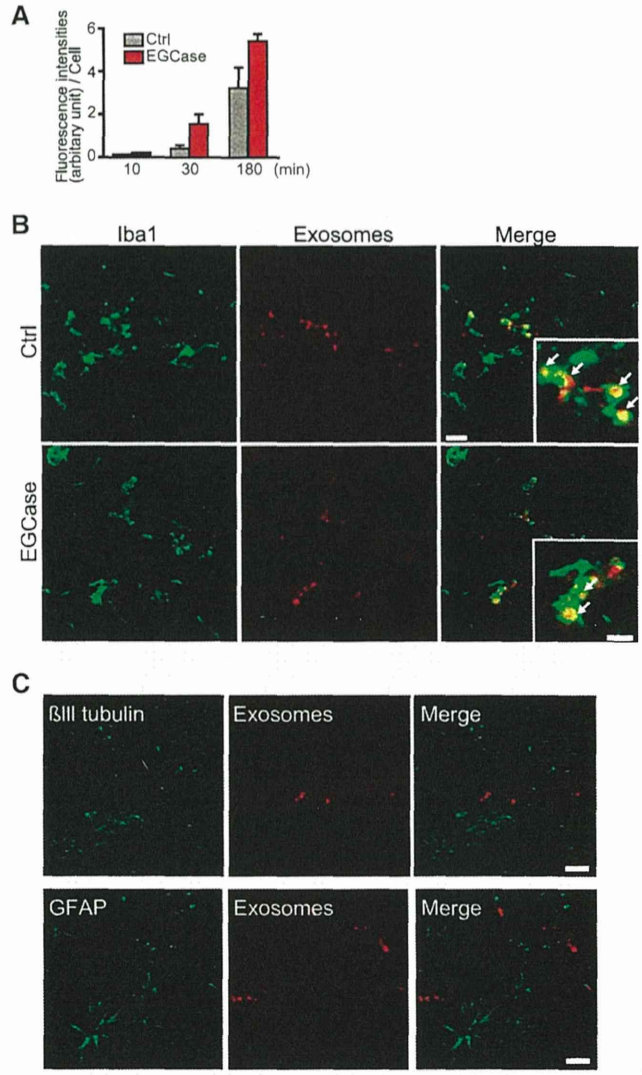

FIGURE 8. **Cleavage of exosomal GSL-glycans does not affect their uptake by microglia.** *A*, fluorescence-labeled exosomes (untreated as Ctrl or treated with EGCase) were exposed to microglial BV-2 cells for 3 h, and the fluorescence intensities of exosomes taken up into the cells were determined by confocal microscopy. *B*, representative hippocampal sections of non-transgenic mice (4 months) injected with fluorescence-labeled exosomes (untreated as Ctrl or treated with EGCase, *red*) and stained with anti-Iba1 antibody. *Arrows* indicate significant exosomal fluorescence in Iba1-positive microglia. *Scale bars*, 50 and 10 μm (*insets*). *C*, hippocampal sections from non-transgenic mice (4 months old) injected with fluorescence-labeled exosomes (untreated as Ctrl or treated with EGCase) stained with antibodies against the neuronal marker βIII tubulin or the astroglial marker glial fibrillary acidic protein (*GFAP*). *Bar*, 50 μm.

and *F*) and demonstrated that Aβs directly bind to the exosomes through the GSL glycans on their surface. Seed-free Aβ was reported to contain soluble species of Aβ but not insoluble amyloid forms (13). The GM1-Aβ complex, which acts as a seed for Aβ amyloidogenesis, is known to consist of a clustered GM1 and a monomeric Aβ molecule (17, 31). Accordingly, our previous report has demonstrated that the exosomes derived from N2a cells almost prevented the oligomeric Aβ formation from seed-free Aβ, but not those preformed Aβ oligomers, which are recognized by A11, a specific antibody against oligomer (8). Thus, the above findings suggested that the exosomes released

from N2a cells would be mostly associated with monomeric Aβ through their surface GSLs. However, a recent study demonstrated that soluble Aβ oligomer strongly binds to GM1-containing membranes *in vitro* and *in vivo*, and GM1-bound Aβ is detected in human cerebrospinal fluid (32). An additional investigation may be required in the future to clarify which form of Aβs can be associated with the exosomes.

It is worth noting that other aggregate-prone proteins, including α-synuclein and prion protein, which cause Parkinson and Creutzfeldt-Jakob diseases, respectively, are also associated with exosomes (33, 34). In addition, α-synuclein and prion protein have been reported to associate with GSLs on the surface of synthetic liposomes (35, 36). A challenging subject of future studies will be determining whether exosomes are involved in the clearance of these proteins.

The normal phagocytotic function of microglia is conceivably important for exosome-bound Aβ clearance in this study. Increasing evidence has indicated that a large portion of secreted exosomes is convincingly taken up by microglia (8, 37). In contrast, a small amount of exosomes can be incorporated into neurons (38). If the clearance function of microglia is decreased or absent, then the exosome-bearing aggregate-prone proteins would trigger pathological events (*i.e.* formation of senile plaque) or even perform minor interneuronal transfer to propagate their toxic assemblies. Indeed, exosome-associated prion proteins, in which their folded species are infectious, can spread between neuronal cells in a monoculture system (33). The transmissibility of amyloids, a characteristic feature of many neurodegenerative diseases including Alzheimer disease and spongiform encephalitis, might emerge under a lack of glial activity for removing exosomes.

Improvement of Aβ clearance by exosome administration or enhancement of exosome generation provides a novel therapeutic approach for AD therapy. It is noteworthy that the Aβ-degrading enzymes, insulin-degrading enzyme and neprilysin, have been reported to be found in exosomes secreted from microglia and adipose tissue-derived mesenchymal stem cells, respectively (39, 40). Exosomes have been used as a delivery platform, encapsulating reagents or siRNAs (41, 42). Peripheral injection of the exosomes holding siRNA (against an APP-processing enzyme, BACE1) succeeded in brain targeting and specific gene knockdown in mice (41). In the future, development of engineered nanovesicles that regulate multiple processes in AD pathogenesis might be a valuable tool for the therapy.

Acknowledgments—Part of this work was conducted at Hokkaido University, supported by "Nanotechnology Platform" Program of the Ministry of Education, Culture, Sports, Science, and Technology (MEXT), Japan.

REFERENCES

1. Scheuner, D., Eckman, C., Jensen, M., Song, X., Citron, M., Suzuki, N., Bird, T. D., Hardy, J., Hutton, M., Kukull, W., Larson, E., Levy-Lahad, E., Viitanen, M., Peskind, E., Poorkaj, P., Schellenberg, G., Tanzi, R., Wasco, W., Lannfelt, L., Selkoe, D., and Younkin, S. (1996) Secreted amyloid β-protein similar to that in the senile plaques of Alzheimer's disease is increased *in vivo* by the presenilin 1 and 2 and APP mutations linked to familial Alzheimer's disease. *Nat. Med.* **2,** 864–870
2. Mawuenyega, K. G., Sigurdson, W., Ovod, V., Munsell, L., Kasten, T., Morris, J. C., Yarasheski, K. E., and Bateman, R. J. (2010) Decreased clearance of CNS β-amyloid in Alzheimer's disease. *Science* **330,** 1774
3. Hardy, J., and Selkoe, D. J. (2002) The amyloid hypothesis of Alzheimer's disease: progress and problems on the road to therapeutics. *Science* **297,** 353–356
4. Simons, M., and Raposo, G. (2009) Exosomes: vesicular carriers for intercellular communication. *Curr. Opin. Cell Biol.* **21,** 575–581
5. Vlassov, A. V., Magdaleno, S., Setterquist, R., and Conrad, R. (2012) Exosomes: current knowledge of their composition, biological functions, and diagnostic and therapeutic potentials. *Biochim. Biophys. Acta* **1820,** 940–948
6. Rajendran, L., Honsho, M., Zahn, T. R., Keller, P., Geiger, K. D., Verkade, P., and Simons, K. (2006) Alzheimer's disease β-amyloid peptides are released in association with exosomes. *Proc. Natl. Acad. Sci. U.S.A.* **103,** 11172–11177
7. Vingtdeux, V., Hamdane, M., Loyens, A., Gelé, P., Drobeck, H., Bégard, S., Galas, M. C., Delacourte, A., Beauvillain, J. C., Buée, L., and Sergeant, N. (2007) Alkalizing drugs induce accumulation of amyloid precursor protein byproducts in luminal vesicles of multivesicular bodies. *J. Biol. Chem.* **282,** 18197–18205
8. Yuyama, K., Sun, H., Mitsutake, S., and Igarashi, Y. (2012) Sphingolipid-modulated exosome secretion promotes clearance of amyloid-β by microglia. *J. Biol. Chem.* **287,** 10977–10989
9. Théry, C., Amigorena, S., Raposo, G., and Clayton, A. (2006) Isolation and characterization of exosomes from cell culture supernatants and biological fluids. *Curr. Protoc. Cell Biol.* **3,** 22
10. DeMattos, R. B., Bales, K. R., Parsadanian, M., O'Dell, M. A., Foss, E. M., Paul, S. M., and Holtzman, D. M. (2002) Plaque-associated disruption of CSF and plasma amyloid-β (Aβ) equilibrium in a mouse model of Alzheimer's disease. *J. Neurochem.* **81,** 229–236
11. Mucke, L., Masliah, E., Yu, G. Q., Mallory, M., Rockenstein, E. M., Tatsuno, G., Hu, K., Kholodenko, D., Johnson-Wood, K., and McConlogue, L. (2000) High-level neuronal expression of Aβ 1–42 in wild-type human amyloid protein precursor transgenic mice: synaptotoxicity without plaque formation. *J. Neurosci.* **20,** 4050–4058
12. Fujitani, N., Furukawa, J., Araki, K., Fujioka, T., Takegawa, Y., Piao, J., Nishioka, T., Tamura, T., Nikaido, T., Ito, M., Nakamura, Y., and Shinohara, Y. (2013) Total cellular glycomics allows characterizing cells and streamlining the discovery process for cellular biomarkers. *Proc. Natl. Acad. Sci. U.S.A.* **110,** 2105–2110
13. Naiki, H., and Gejyo, F. (1999) Kinetic analysis of amyloid fibril formation. *Methods Enzymol.* **309,** 305–318
14. Théry, C. (2011) Exosomes: secreted vesicles and intercellular communications. *F1000 Biol. Rep.* **3,** 15
15. Grapp, M., Wrede, A., Schweizer, M., Hüwel, S., Galla, H. J., Snaidero, N., Simons, M., Bückers, J., Low, P. S., Urlaub, H., Gärtner, J., and Steinfeld, R. (2013) Choroid plexus transcytosis and exosome shuttling deliver folate into brain parenchyma. *Nat. Commun.* **4,** 2123
16. Ariga, T., McDonald, M. P., and Yu, R. K. (2008) Role of ganglioside metabolism in the pathogenesis of Alzheimer's disease: a review. *J. Lipid Res.* **49,** 1157–1175
17. Utsumi, M., Yamaguchi, Y., Sasakawa, H., Yamamoto, N., Yanagisawa, K., and Kato, K. (2009) Up-and-down topological mode of amyloid β-peptide lying on hydrophilic/hydrophobic interface of ganglioside clusters. *Glycoconj. J.* **26,** 999–1006
18. Yanagisawa, K., Odaka, A., Suzuki, N., and Ihara, Y. (1995) GM1 ganglioside-bound amyloid β-protein (A β): a possible form of preamyloid in Alzheimer's disease. *Nat. Med.* **1,** 1062–1066
19. Hayashi, H., Kimura, N., Yamaguchi, H., Hasegawa, K., Yokoseki, T., Shibata, M., Yamamoto, N., Michikawa, M., Yoshikawa, Y., Terao, K., Matsuzaki, K., Lemere, C. A., Selkoe, D. J., Naiki, H., and Yanagisawa, K. (2004) A seed for Alzheimer amyloid in the brain. *J. Neurosci.* **24,** 4894–4902
20. Fujitani, N., Takegawa, Y., Ishibashi, Y., Araki, K., Furukawa, J., Mitsutake, S., Igarashi, Y., Ito M., and Shinohara, Y. (2011) Qualitative and quantitative cellular glycomics of glycosphingolipids based on rhodococcal endoglycosylceramidase-assisted glycan cleavage, glycoblotting-assisted

sample preparation, and matrix-assisted laser desorption ionization tandem time-of-flight mass spectrometry analysis. *J. Biol. Chem.* **286,** 41669–41679
21. Yanagisawa, K., and Matsuzaki, K. (2002) Cholesterol-dependent aggregation of amyloid β-protein. *Ann. N.Y. Acad. Sci.* **977,** 384–386
22. Yuyama, K., and Yanagisawa, K. (2010) Sphingomyelin accumulation provides a favorable milieu for GM1 ganglioside-induced assembly of amyloid β-protein. *Neurosci. Lett.* **481,** 168–172
23. Trajkovic, K., Hsu, C., Chiantia, S., Rajendran, L., Wenzel, D., Wieland, F., Schwille, P., Brügger, B., and Simons, M. (2008) Ceramide triggers budding of exosome vesicles into multivesicular endosomes. *Science* **319,** 1244–1247
24. Takata, K., Hirata-Fukae, C., Becker, A. G., Chishiro, S., Gray, A. J., Nishitomi, K., Franz, A. H., Sakaguchi, G., Kato A., Mattson, M. P., Laferla, F. M., Aisen, P. S., Kitamura, Y., and Matsuoka, Y. (2007) Deglycosylated anti-amyloid β antibodies reduce microglial phagocytosis and cytokine production while retaining the capacity to induce amyloid β sequestration. *Eur. J. Neurosci.* **26,** 2458–2468
25. Gulbins, E., and Kolesnick, R. (2003) Raft ceramide in molecular medicine. *Oncogene* **22,** 7070–7077
26. Simons, K., and Ikonen, E. (1997) Functional rafts in cell membranes. *Nature* **387,** 569–572
27. de Gassart, A., Geminard, C., Fevrier, B., Raposo, G., and Vidal, M. (2003) Lipid raft-associated protein sorting in exosomes. *Blood* **102,** 4336–4344
28. Keilani, S., Lun, Y., Stevens, A. C., Williams, H. N., Sjoberg, E. R., Khanna, R., Valenzano, K. J., Checler, F., Buxbaum, J. D., Yanagisawa, K., Lockhart, D. J., Wustman, B. A., and Gandy, S. (2012) Lysosomal dysfunction in a mouse model of Sandhoff disease leads to accumulation of ganglioside-bound amyloid-β peptide. *J. Neurosci.* **32,** 5223–5236
29. Xu, Y. H., Barnes, S., Sun, Y., and Grabowski, G. A. (2010) Multi-system disorders of glycosphingolipid and ganglioside metabolism. *J. Lipid Res.* **51,** 1643–1675
30. Bolmont, T., Haiss, F., Eicke, D., Radde, R., Mathis, C. A., Klunk, W. E., Kohsaka, S., Jucker, M., and Calhoun, M. E. (2008) Dynamics of the microglial/amyloid interaction indicate a role in plaque maintenance. *J. Neurosci.* **28,** 4283–4292
31. Matsuzaki, K., Kato, K., and Yanagisawa, K. (2010) Aβ polymerization through interaction with membrane gangliosides. *Biochim. Biophys. Acta* **1801,** 868–877
32. Hong, S., Ostaszewski, B. L., Yang, T., O'Malley, T. T., Jin, M., Yanagisawa, K., Li, S., Bartels, T., and Selkoe, D. J. (2014) Soluble Aβ oligomers are rapidly sequestered from brain ISF *in vivo* and bind GM1 ganglioside on cellular membranes. *Neuron* **82,** 308–319
33. Fevrier, B., Vilette, D., Archer, F., Loew, D., Faigle, W., Vidal, M., Laude, H., and Raposo, G. (2004) Cells release prions in association with exosomes. *Proc. Natl. Acad. Sci. U.S.A.* **101,** 9683–9688
34. Emmanouilidou, E., Melachroinou, K., Roumeliotis, T., Garbis, S. D., Ntzouni, M., Margaritis, L. H., Stefanis, L., and Vekrellis, K. (2010) Cell-produced α-synuclein is secreted in a calcium-dependent manner by exosomes and impacts neuronal survival. *J. Neurosci.* **30,** 6838–6851
35. Martinez, Z., Zhu, M., Han, S., and Fink, A. L. (2007) GM1 specifically interacts with α-synuclein and inhibits fibrillation. *Biochemistry* **46,** 1868–1877
36. Sanghera, N., Correia, B. E., Correia, J. R., Ludwig, C., Agarwal, S., Nakamura, H. K., Kuwata, K., Samain, E., Gill, A. C., Bonev, B. B., and Pinheiro, T. J. (2011) Deciphering the molecular details for the binding of the prion protein to main ganglioside GM1 of neuronal membranes. *Chem. Biol.* **18,** 1422–1431
37. Fitzner, D., Schnaars, M., van Rossum, D., Krishnamoorthy, G., Dibaj, P., Bakhti, M., Regen, T., Hanisch, U. K., and Simons, M. (2011) Selective transfer of exosomes from oligodendrocytes to microglia by macropinocytosis. *J. Cell Sci.* **124,** 447–458
38. Frühbeis, C., Fröhlich, D., Kuo, W. P., Amphornrat, J., Thilemann, S., Saab, A. S., Kirchhoff, F., Möbius, W., Goebbels, S., Nave, K. A., Schneider, A., Simons, M., Klugmann, M., Trotter, J., and Krämer-Albers, E. M. (2013) Neurotransmitter-triggered transfer of exosomes mediates oligodendrocyte-neuron communication. *PLoS Biol.* **11,** e1001604
39. Tamboli, I. Y., Barth, E., Christian, L., Siepmann, M., Kumar, S., Singh, S., Tolksdorf, K., Heneka, M. T., Lütjohann, D., Wunderlich, P., and Walter, J. (2010) Statins promote the degradation of extracellular amyloid β-peptide by microglia via stimulation of exosome-associated insulin-degrading enzyme (IDE) secretion. *J. Biol. Chem.* **285,** 37405–37414
40. Katsuda, T., Tsuchiya, R., Kosaka, N., Yoshioka, Y., Takagaki, K., Oki, K., Takeshita, F., Sakai, Y., Kuroda, M., and Ochiya, T. (2013) Human adipose tissue-derived mesenchymal stem cells secrete functional neprilysin-bound exosomes. *Sci. Rep.* **3,** 1197
41. Alvarez-Erviti, L., Seow, Y., Yin, H., Betts, C., Lakhal, S., and Wood, M. J. (2011) Delivery of siRNA to the mouse brain by systemic injection of targeted exosomes. *Nat. Biotechnol.* **29,** 341–345
42. Zhuang, X., Xiang, X., Grizzle, W., Sun, D., Zhang, S., Axtell, R. C., Ju, S., Mu, J., Zhang, L., Steinman, L., Miller, D., and Zhang, H. G. (2011) Treatment of brain inflammatory diseases by delivering exosome encapsulated anti-inflammatory drugs from the nasal region to the brain. *Mol. Ther.* **19,** 1769–1779

OPEN ACCESS Freely available online

PLOS | ONE

Generation of Human Induced Pluripotent Stem (iPS) Cells in Serum- and Feeder-Free Defined Culture and TGF-β1 Regulation of Pluripotency

Sachiko Yamasaki[1], Yuki Taguchi[1], Akira Shimamoto[2], Hanae Mukasa[1], Hidetoshi Tahara[2], Tetsuji Okamoto[1]*

1 Department of Molecular Oral Medicine and Maxillofacial Surgery, Applied Life Sciences, Graduate Institute of Biomedical & Health Sciences, Hiroshima University, Japan, **2** Department of Cellular and Molecular Biology, Basic Life Sciences, Graduate Institute of Biomedical & Health Sciences, Hiroshima University, Japan

Abstract

Human Embryonic Stem cells (hESCs) and human induced Pluripotent Stem cells (hiPSCs) are commonly maintained on inactivated mouse embryonic fibroblast as feeder cells in medium supplemented with FBS or proprietary replacements. Use of culture medium containing undefined or unknown components has limited the development of applications for pluripotent cells because of the relative lack of knowledge regarding cell responses to differentiating growth factors. In addition, there is no consensus as to the optimal formulation, or the nature of the cytokine requirements of the cells to promote their self-renewal and inhibit their differentiation. In this study, we successfully generated hiPSCs from human dental pulp cells (DPCs) using Yamanaka's factors (*Oct3/4, Sox2, Klf4,* and *c-Myc*) with retroviral vectors in serum- and feeder-free defined culture conditions. These hiPSCs retained the property of self-renewal as evaluated by the expression of self-renewal marker genes and proteins, morphology, cell growth rates, and pluripotency evaluated by differentiation into derivatives of all three primary germ layers *in vitro* and *in vivo*. In this study, we found that TGF-β1 increased the expression levels of pluripotency markers in a dose-dependent manner. However, increasing doses of TGF-β1 suppressed the growth rate of hiPSCs cultured under the defined conditions. Furthermore, over short time periods the hiPSCs cultured in hESF9 or hESF9T exhibited similar morphology, but hiPSCs maintained in hESF9 could not survive beyond 30 passages. This result clearly confirmed that hiPSCs cultured in hESF9 medium absolutely required TGF-β1 to maintain pluripotency. This simple serum-free adherent monoculture system will allow us to elucidate the cell responses to growth factors under defined conditions and can eliminate the risk might be brought by undefined pathogens.

Citation: Yamasaki S, Taguchi Y, Shimamoto A, Mukasa H, Tahara H, et al. (2014) Generation of Human Induced Pluripotent Stem (iPS) Cells in Serum- and Feeder-Free Defined Culture and TGF-β1 Regulation of Pluripotency. PLoS ONE 9(1): e87151. doi:10.1371/journal.pone.0087151

Editor: Zhongjun Zhou, The University of Hong Kong, Hong Kong

Received August 30, 2013; **Accepted** December 19, 2013; **Published** January 29, 2014

Funding: This work was supported in part by research grants (no. 22659369 and 24890139) from the Japanese Ministry of Education, Culture, Sports, Science and Technology to TO and SY. The funders had no role in study design, data collection and analysis, decision to publish, or preparation of the manuscript.

Competing Interests: The authors have declared that no competing interests exist.

* E-mail: tetsuok@hiroshima-u.ac.jp

Introduction

Human somatic cells can be reprogrammed into induced pluripotent stem cells (iPSCs) by introduction of transcription factors such as *Oct3/4*, *Sox2*, *Klf4* and *c-Myc* [1]. Embryonic stem cells (ESCs) and human iPSCs (hiPSCs) can proliferate without limit and yet maintain the potential to generate derivatives of all three germ layers. These properties make them useful for understanding the basic biology of the human body, for drug discovery and testing, and for transplantation therapies. However, the original protocol for the derivation of hiPSCs required feeder cells and mouse embryonic fibroblasts (MEF) to provide a microenvironment for the reprogramming and the maintenance of hiPSCs [1,2]. Although it is known that MEFs produce a number of secreted protein factors, they are traditionally used for ES cell culture. The inclusion of uncharacterized animal protein supplements makes culture conditions more complex with increased variability in nutrients and factors that contribute to cell growth and the maintenance of pluripotency. Furthermore there is unavoidable variability in using live cells as feeders, which may affect reprogramming steps. For these reasons defined culture conditions without feeder cells are desirable. Although several defined culture conditions without feeder cells for hiPSCs have been reported, manipulation of undifferentiated hESCs and hiPSCs still remains problematic. For example, as we show below, hiPSCs cultured in serum-free and feeder-free conditions in the absence of exogenous TGF-β1 lose pluripotency with passaging over time.

Previously, feeder-free methods using FGF-2 and activin A for iPS cell derivation from adult fibroblasts using hESF9 medium [3] (Table S1) or using chemically defined conditions for hiPS cell derivation and culture [4] have been reported. In the present study, we adapted a method that has been established for hES cell culture, which uses FGF-2 and heparin with a defined medium formulation [5]. We have validated the same formula in the reprogramming of fetal lung fibroblasts (TIG-3) and adult dental pulp cells (DPCs) to iPSCs without feeder cells. At first, we examined whether hESF9 medium and each of three ECM (type I collagen, gelatin, fibronectin) -coated surfaces could be used for iPS cell derivation. Although each ECM could generate hiPSCs,

type I collagen and gelatin could not maintain the pluripotency of hiPSCs. Secondly, we performed retrovirus production using PLAT-A cells in serum-free conditions and analyzed transduction efficiency. From these results, we performed hiPS cell generation from patient-derived DPCs using hESF9 medium with fibronectin in completely serum-free culture conditions. The medium is capable of maintaining reprogrammed cells that expressed ES cell factors and retained the potential to differentiate into all three embryonic germ layers.

TGF-βs and their family members have been implicated in the development and maintenance of various organs in which stem cells play important roles. In hESCs, the predominant signaling pathways involved in pluripotency and self-renewal are TGF-β, which signals through Smad2, 3, 4, and FGFR, which activates the MAPK and Akt pathways. Signaling through these pathways results in the expression and activation of three key transcription factors: Oct3/4, Sox2, and Nanog. These transcription factors activate gene expression of ESC-specific genes, regulate their own expression and also serve as hESCs markers. To improve the stability of hiPSC pluripotency, we investigated the effect of TGF-β1. The addition of TGF-β1 to the defined serum-free medium for hiPSCs supported the robust proliferation and continued pluripotency of hiPSCs. Here we show that hESF9 medium in completely defined serum-free culture conditions supports the derivation and maintenance of pluripotent stem cells. This culture system will allow us to elucidate the cell responses to growth factors under defined conditions. These advantages will be beneficial for clarifying the molecular mechanisms of early development.

Materials and Methods

Ethics Statement

Written approval for human tissue collection and subsequent iPS cell generation and genome/gene analyses performed in this study was obtained from the Ethics Committee for Human Genome/Gene Analysis Research at Hiroshima University (approval number: hi-58), and written informed consent was obtained from each individual patient. All animal experiments in this study strictly followed a protocol approved by the Institutional Animal Care and Use Committee of Hiroshima University (approval number: A-11-140).

Cell culture of Dental pulp cell

Using a protocol approved by the Ethics Committee for Human Genome/Gene Analysis Research at Hiroshima University, we collected normal human third molars at Hiroshima University Hospital after having obtained informed consent for the usage of dental pulp cells (DPCs) to derive iPSCs. Primary human dental pulp cell cultures were established from dental pulp tissue discarded during surgery. The pulp tissue samples were minced into small clumps and then transferred into type I collagen (0.15 mg/ml) (Nitta gelatin, Osaka, Japan)- coated culture dishes in RD6F serum-free medium [11,12]. The cells were cultured at 37°C in a humid atmosphere of 5% CO_2. Fibroblastic cells that grew out from these colonies were digested in 0.05% trypsin-ethylenediaminetetraacetic acid (EDTA) in Ca^{2+} and Mg^{2+}-free phosphate-buffered saline (PBS), and the trypsin was inactivated with 0.1% soybean trypsin inhibitor (Sigma Aldrich, St. Louis, MO) in PBS. These cells were subcultured every 2-3 day.

Retrovirus production using PLAT-A packaging cell line

PLAT-A packaging cells [6] (Cell Bio Labs Inc., San Diego, CA) were seeded at 2×10^6 cells on collagen-coated flasks and cultured overnight in DMEM supplemented with 10% FBS. The next day, pMXs retroviral vectors (Add Gene, Cambridge, MA) containing the open reading frames of *Oct3/4*, *Sox2*, *Klf4*,*c-Myc* and *EGFP* were transfected into PLAT-A cells with Xtreme GENE HP Transfection Reagent (Roche Diagnostics, Cambridge, MA). After 48 hr the medium was completely changed to serum-free hESF9. Viral supernatants were collected 48 h to 72 h after transfection, filtered through a 0.45 μm pore size PVDF filter (Millex-HV, Millipore, Billerica, MA) and supplemented with 8 μg/ml Polybrene (Sigma). The DPCs were transduced with *Oct3/4:Sox2:Klf4:c-Myc* (1:1:1:1) mixture of viral supernatant. To determine the viral transduction efficiency of individual factors, *EGFP* transduced retrovirus supernatant was transduced to DPCs. Medium was changed every other day, and the cells cultured for 4 days. The cells were trypsinized and analyzed by flow cytometry (FACS Calibur™) (BD Biosciences, San Jose, CA).

The generation of hiPS cell using TIG-3 under feeder- and serum-free, defined culture conditions from the reprogramming step

To obtain iPSCs, TIG-3 (derived from fetal lung fibroblasts and purchased from the Health Science Research Resources Bank, Osaka, Japan) [7] cultured in DMEM supplemented with 10% FBS were transduced with the pMXs-based retroviral vectors encoding human *Oct3/4*, *Sox2*, *Klf4* and *c-Myc*, as described above. At the same time, TIG-3 were transduced the EGFP-expressing retroviral vector or the control vector with a constant amount of total DNA. After 4 days cells were photographed under a fluorescence microscope and analyzed by flow cytometry (FACS Calibur™). After 4 days cells transduced with the four factors were trypsinized and plated on 0.1% gelatin- (Millipore), or type I collagen- (0.3 mg/ml) (Nitta gelatin) or fibronectin- (2 μg/cm^2) (Sigma) coated dishes in hESF9 medium. For comparison, we used KSR-based medium and mitomycin C-treated MEF (Embryo Max® PMEF-H, Millipore) [8–10] as feeder cells (KSR-based conditions)[1,2]. After 20 days, we detected colonies that were subsequently passaged and maintained in hESF9 medium with individual ECMs. After 36 days of culture, ALP–positive colonies were counted.

Retrovirus Production using PLAT-A cell in serum-free conditions and transduction efficiency

Retroviral supernatants of pMXs-(empty) and pMXs-(EGFP) were produced in PLAT-A packaging cells in hESF9 medium or DMEM supplemented with 10% FBS. These collected virus supernatants were used for infection. After 3 days, infected TIG-3 cells were photographed under a fluorescence microscope and transduction efficiency analyzed by FACS Calibur™ of EGFP expression.

Generation of hiPS Cells from DPCs in completely defined culture conditions

DPCs were seeded at 3×10^5 cells per 60-mm dish in RD6F serum-free medium [11,12] and cultured overnight. The next day the cells were infected with viral supernatant for 24 h in hESF9 medium. Four days after transduction, these infected cells were harvested by trypsinization and seeded on fibronectin (2 μg/cm^2) (Sigma F-1141) -coated dishes at 1×10^5 cells per 100 mm dish in hESF9-medium. The medium was changed every other day. Approximately 20 days after infection, iPS colonies were picked based on human ES cell-like colony morphology. The picked colonies were subsequently expanded and maintained on fibronectin in hESF9T medium. Reprogramming efficiency was determined as the positive number of total ES-like ALP positive

colonies per total number of infected cells. Thirty-three days after transduction, we detected hiPSC-like colonies by ALP substrate staining. As a control, transduced DPCs were seeded on mitomycin-C-treated MEF feeder cells with KSR-based conditions [1,2].

Maintenance of human iPS cells in serum-free culture conditions

For subculturing colonies were mechanically detached from the culture dish and dissociated into small clamps by pipetting. The cell suspension was transferred on fibronectin-coated dishes in hESF9 medium or hESF9 with TGF-β1 (2 ng/ml) (R&D systems, Minneapolis, MN) (hESF9T). We defined this stage as passage 1. The medium was changed daily with hESF9T medium.

Cell growth analysis of human iPS cells generated and maintained in define culture conditions

Human iPSCs generated under hESF9 and cultured in hESF9T (DP-F-iPS-CL8 passage 38, DP-F-iPS-CL4 passage 38, DP-F-iPS-CL16 passage 33) were seeded in a 24-well plate coated with fibronectin and counted every 24 hr. Growth curves were calculated from each passage split ratio. The hiPSC colonies (DP-F-iPSCs) cultured for 1 month in feeder-free hESF9 or hESF9T were detached using a cell scraper and 0.001% trypsin-0.01% ethylenediaminetetraacetic acid (EDTA). The dissociated cells were then fixed, incubated with Alexa Fluor 647®-conjugated SSEA4 antibody or PerCP-Cy5.5-conjugated Oct3/4, and subjected to flow cytometry (FACS Aria™).

Alkaline phosphate (ALP) staining and Immunocytochemistry

Alkaline phosphatase staining was performed using a Fast Red substrate kit (Nichirei Biosciences Inc., Tokyo, Japan). To detect pluripotent stem cell marker antigens cells were fixed with PBS containing 4% paraformaldehyde for 10 min at room temperature. After washing with PBS, the cells were treated with PBS containing 5% normal goat serum (Nichirei) and 0.1% Triton X-100 for 45 min at room temperature. Fixed cells were stained with primary antibodies included SSEA-4 (1:100, Stemgent®, Cambridge, MA), TRA-1-60 (1/200, Stemgent®), TRA-1-81 (1/200, Stemgent®), Oct-3/4 (1/200 Millipore), Nanog (1/600, ReproCELL, Yokohama, Japan), Nestin (1/200, Millipore), βIII-tubulin (1/200, Millipore), α-smooth muscle actin (pre-diluted, DAKO Cytomation, Glostrup, Denmark) and α-fetoprotein (1/100, R&D Systems). These primary antibodies were visualized with Alexa Fluor® 488- conjugated goat anti-rabbit IgG, or Alexa Fluor® 594-conjugated goat anti-rabbit IgG, or Alexa Fluor® 488-conjugated goat anti-mouse IgG, or Alexa Fluor® 594-conjugated goat anti-mouse IgG (1/200, Invitrogen, Carlsbad, CA). Nucleuses were stained with DAPI. Fluorescence images were acquired using a Zeiss inverted LSM confocal microscope (Carl Zeiss, GmbH, Germany).

RNA isolation and reverse transcription gene expression

A detailed reverse transcription-polymerase chain reaction (RT-PCR) protocol was described previously [13]. Briefly, total RNA was extracted from iPSCs using the Illustra RNA spin Mini Isolation kit (GE Healthcare UK Ltd, Buckinghamshire, England), according to manufacturer's instructions. cDNA was synthesized from 1 μg of total RNA using High capacity RNA-to cDNA master mix (Applied Biosystems, Carlsbad, CA). RT-PCR was performed with AmpliTaq Gold DNA polymerase with Gene Amp (Applied Biosystems). The primers used in this study are described in Table S2. PCR products were size-fractionated using 1.5% agarose gel electrophoresis. DNA markers were used to confirm the size of the fragments.

Droplet digital PCR analysis

Droplet digital PCR (ddPCR) analysis was performed using QX100™ Droplet Digital™ PCR (Bio-RAD Laboratories, Hercules, CA). Total RNA was extracted from hiPSCs, and RT-PCR was performed. cDNA samples, primers and probes with the ddPCR master mix (Bio-Rad) were combined in water-oil emulsion droplets. These droplets were subjected to 40 PCR cycles. Positive and negative fluorescent droplets in each sample were detected with a QX100 Droplet reader (Bio-Rad). The relative mRNA expression in each sample was normalized to its GAPDH content. The mRNA levels in each cells were expressed relative to those in hESF9 medium (TGF-β1; 0 ng/ml), which was taken as 1. The results are presented as means±SD of three independent experiments.

Embryoid body formation

In vitro differentiation was induced by the formation of embryoid bodies as described previously [5]. Briefly, undifferentiated human DP-iPSCs were cultured in DMEM with 10% FBS for 4 days in low-attachment 96 well plates. After 4 days in suspension culture, floating embryoid bodies were re-seeded onto gelatin-coated dishes in the same culture medium for 10 days. The medium was changed every other day.

Teratoma formation assay and histological analysis

Human DP-iPSCs were suspended at 2×10^7 cells/ml in PBS and injected 50 ul of the cell suspension (1×10^6 cells) subcutaneously into dorsal flank of SCID (CB17/Icr-*Prkdc*^{scid}/CrlCrlj) mice. Ten weeks after the injection, tumors were surgically dissected from the mice. Teratomas were weighed, fixed in PBS containing 4% formaldehyde, and embedded in paraffin. Sections were stained with hematoxylin and eosin and Alcian Blue stain.

Short tandem repeat DNA analysis

Genomic DNA was used for PCR with Powerplex 16 system (Promega Corporation, Madison, WI) and analyzed by ABI PRISM 3100 Genetic analyzer and Gene Mapper v3.5 (Applied Biosystems).

RNA expression array analysis

A heat map generated from the RNA expression array data displayed the expression profile of the hESC-enriched genes and the differentiated cell-enriched genes. The genes shown in blue represented the down-regulation of gene expression, whereas the genes shown in red represented the up-regulation of gene expression. RNA expression array were performed using the Agilent Sure Print G3 Human GE 8x60K v2 Microarray, and data were analyzed using Genespring12.0 (Agilent Technologies, Santa Clara, CA).

Results

The generation of hiPS cells using TIG-3 under feeder- and serum-free, defined culture conditions from the reprogramming step

We examined whether hESF9 medium and each of three ECM (type I collagen, gelatin, fibronectin)-coated surfaces could be used for iPS cell derivation. We used Platinum-A retroviral packaging cell, amphotropic (PLAT-A) [6] carrying the *Oct3/4, Sox2, Klf4*

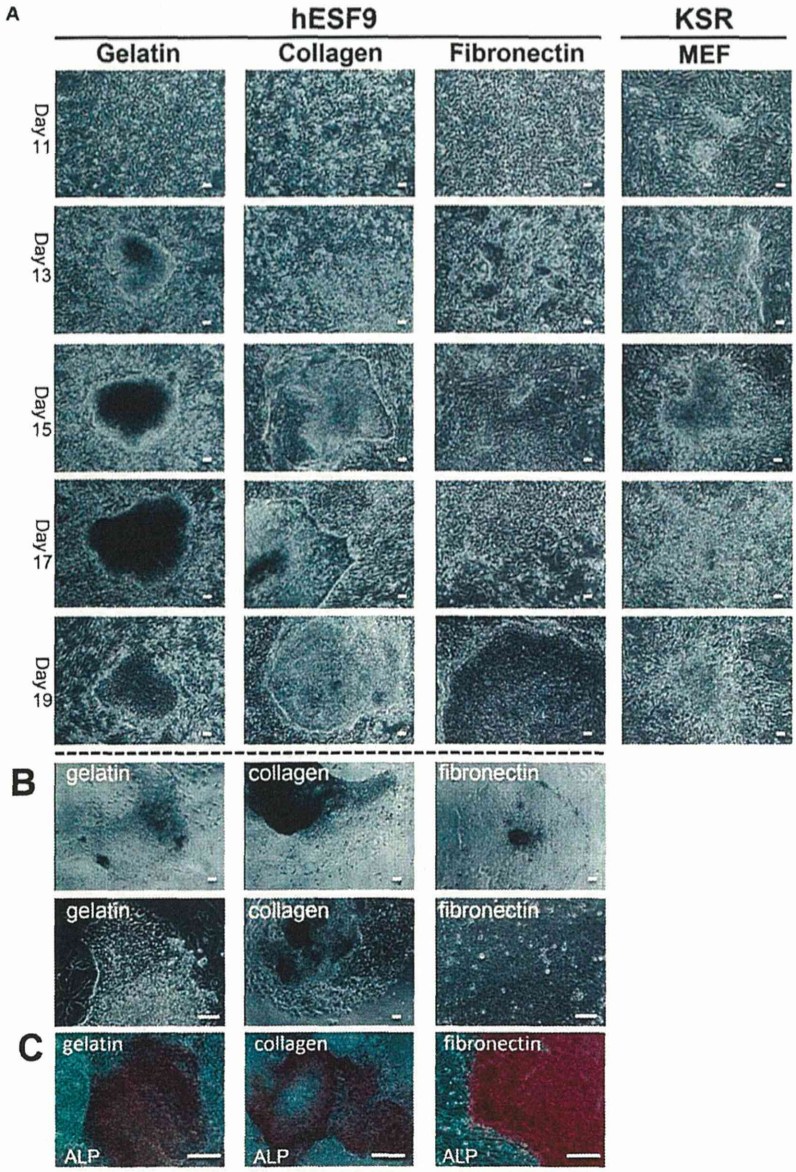

Figure 1. Morphology of transduced TIG-3 on each ECMs in hESF9 medium. A) Transduced TIG-3 cells were cultured on each ECMs with hESF9 medium or on MEF with KSR-based conditions. After 20 days, iPS colony were picked up and sub-cultured on each ECMs. B) Images of sub-cultured iPS colonies seeded after 2days on each ECMs with hESF9 medium. C) ALP staining of iPSCs on gelatin, collagen, and fibronectin (infect after 36days). Bars indicate 200 μm.
doi:10.1371/journal.pone.0087151.g001

and *c-Myc* in DMEM supplemented with 10% FBS. We produced retroviruses using PLAT-A cell line in serum-supplemented conditions as described in the manufacture's protocol. Then we transduced four factors (*Oct3/4*, *Sox2*, *Klf4* and *c-Myc*) into TIG-3 (normal fibroblast cell line derived from fetal lung) [7] in DMEM supplemented with 10% FBS. At the same time, we transfected the EGFP-expressing retroviral vector and the empty control vector into TIG-3 with a constant amount of total DNA. After 4 days, cells were photographed under a fluorescence microscope and analyzed by flow cytometry. The transduction efficiency of the four factors was 26.6% as measured by EGFP expression (Fig. S1). After 4 days four factor-transduced cells were trypsinized and plated on 0.1% gelatin, or type I collagen (0.3 mg/ml) or fibronectin (2 μg/cm^2) in hESF9 medium. For comparison, we used KSR-based medium and mitomycin C-treated MEF [8-10] feeder cells (KSR-based conditions) [1,2]. After 13 days of culture, we observed human ES-like colonies, characterized by large nuclei and little cytoplasm (Fig. 1-A). After 20 days colonies were passaged and maintained in hESF9 medium on substrates coated with individual ECMs (Fig. S2-A). After 36 days of culture, alkaline phosphatase (ALP)–positive colonies were counted, and relatively high iPS induction efficiency was observed. However, although type I collagen supported hiPS cell generation more effectively than the other two ECMs, collagen and gelatin did not

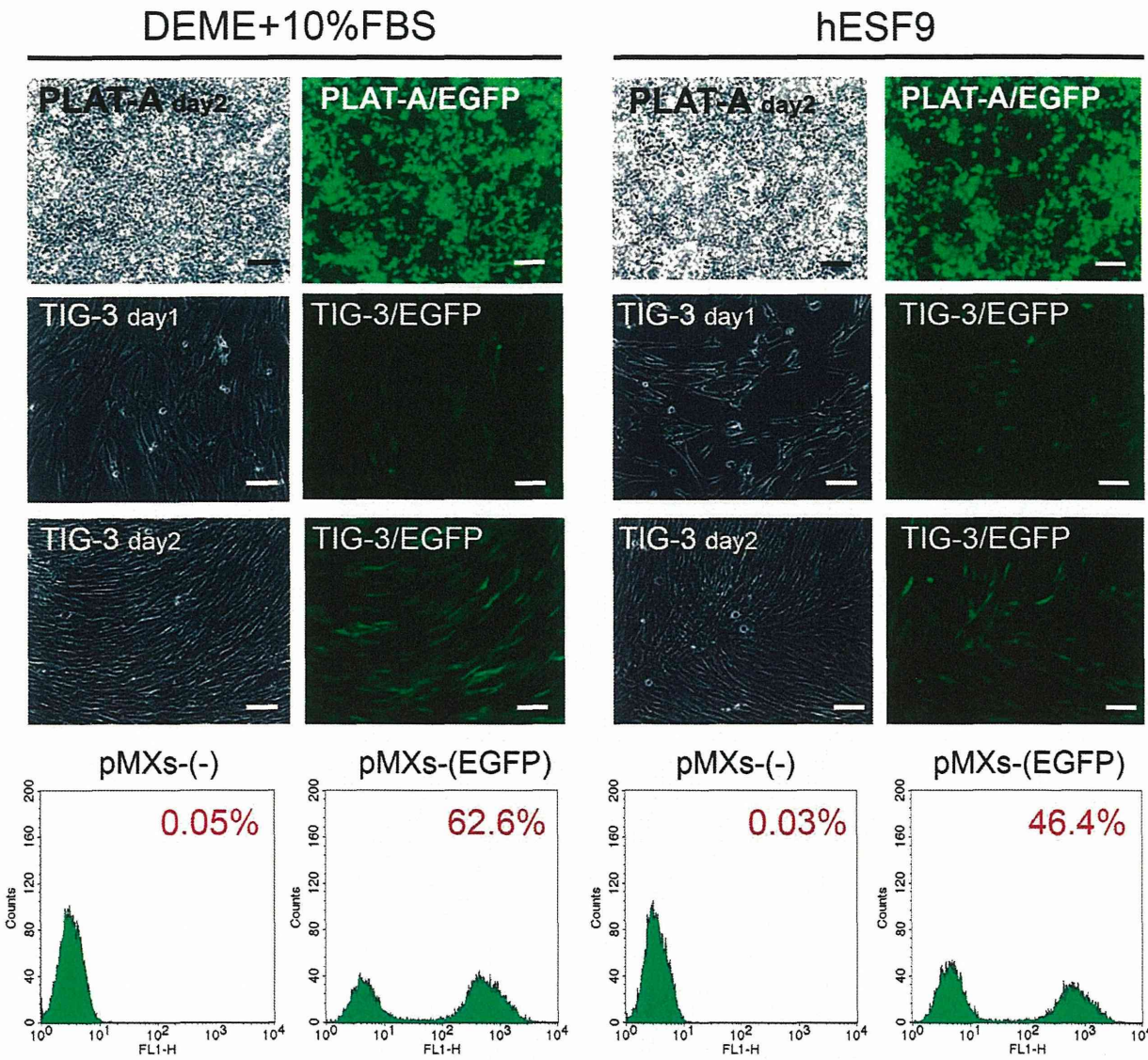

Figure 2. Transduction efficiency of retroviruses in serum-free hESF9 medium and serum-supplemented medium in TIG-3. TIG-3 was introduced with pMXs retroviruses containing the EGFP cDNA. After 3 days, cells were photographed under a fluorescence microscope and analyzed by flow cytometry. The left panel shows the images of phase contrast, fluorescent microscope and the results of flow cytometry of the cells cultured in serum-supplemented condition (DMEM+10%FBS). The right panel shows the cells in serum-free culture conditions (hESF9). Transfection efficiency of EGFP was 62.6% in serum-supplemented condition and 46.4% in serum-free culture condition. Bars indicate 200 μm.
doi:10.1371/journal.pone.0087151.g002

support pluripotency of hiPSCs after further culture of these colonies (Fig.1-B). This inability to maintain pluripotency of hiPSCs was confirmed by ALP activity (Fig.1-C) and RT-PCR analysis (Fig. S2-B).

Retrovirus production using PLAT-A cell in serum-free conditions and analysis of transduction efficiency

We examined whether the serum-free culture condition could produce relatively high titer viral supernatants. Retroviral supernatants of pMXs-(empty) and pMXs-(EGFP) were produced in PLAT-A packaging cells in serum-free hESF9 medium or serum supplemented medium. The collected virus supernatants were used for infection. After 3 days, transduction efficiency was measured by FACS analysis of EGFP expression. Transduction efficiency in serum-free hESF9 medium was 46.4%, whereas it was 62.6% in serum-supplemented medium (Fig. 2, Fig. S3). While the data showed a slightly lower titer in hESF9, the viral titer was sufficient to reprogram dental pulp cells (see below).

hiPS cell generation from adult DPCs in serum- and feeder-free culture condition

We obtained dental pulp cells (DPCs) from healthy patients (Fig. 3, Fig. S4). These DPCs were reprogrammed to hiPSCs after transduction with PLAT-A virus in completely serum-free culture conditions (Fig. 3). The transduced DPCs were trypsinized and plated on fibronectin-coated dish in hESF9 medium. Human iPS

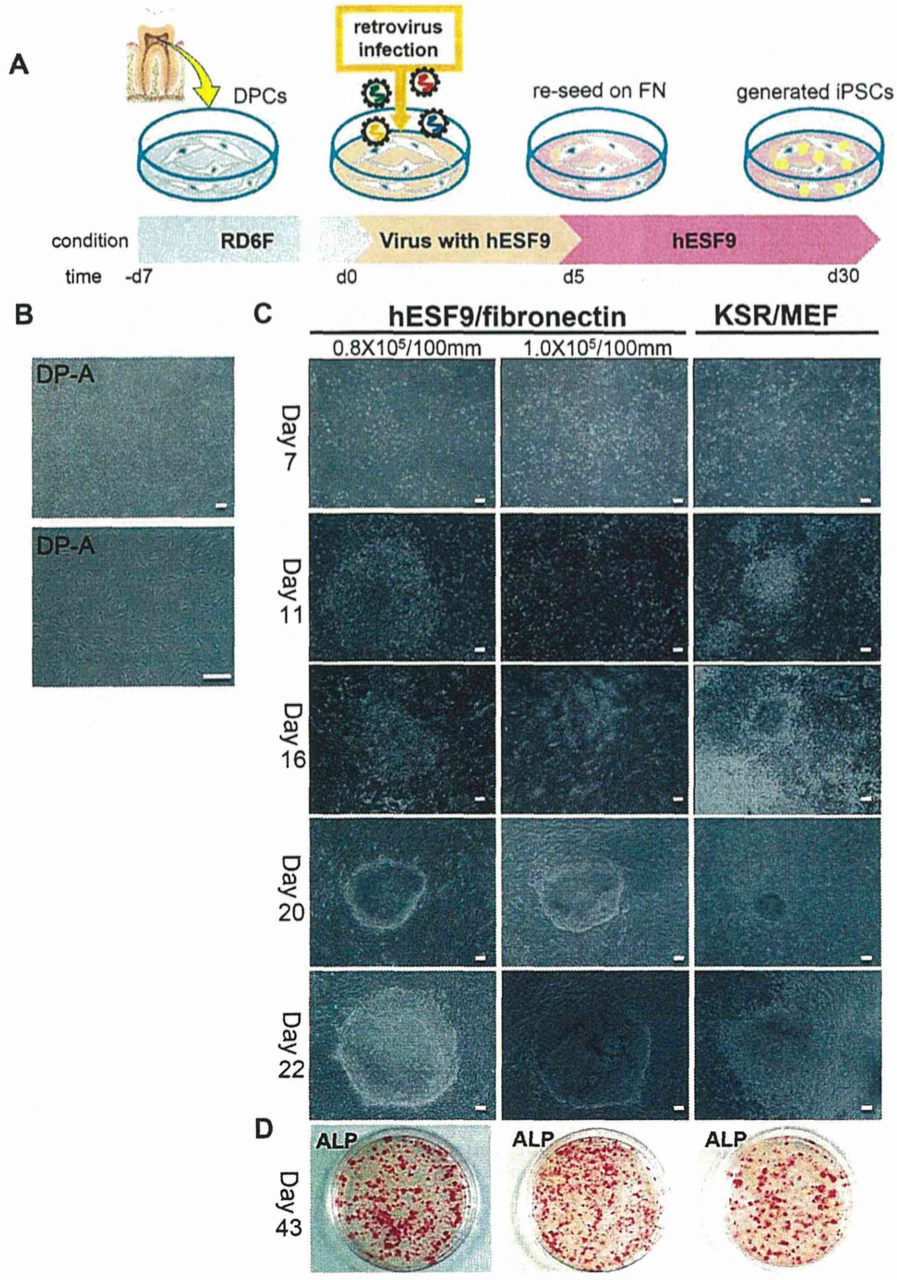

Figure 3. hiPSC generation from DPCs in serum- and feeder-free culture conditions. A) Time schedule of hiPSC generation. Day-7~0: DPCs were cultured in RD6F serum-free medium on type I collagen-coated dish. Day 0~4: Retroviral transduction (*Oct3/4, Sox2, KLF-4, c-Myc*) with hESF9 medium. Day5: re-seeding on fibronectin-coated plate with hESF9 medium. Day6~30: replace medium every other day. B) Images of DPCs (DP-A: passage 4) on type I collagen-coated plate with RD6F medium. C) Transduced DPCs were cultured on fibronectin with hESF9 medium or on MEF with KSR-based conditions. After 20 days, iPS colony were picked up and sub-cultured on fibronectin. The reprogramming efficiency was 0.23–0.38% with a high success rate. D) ALP staining of iPSCs on fibronectin, 43 days after infection. Bars indicate 200 μm.
doi:10.1371/journal.pone.0087151.g003

cell colonies intermingled with partially reprogrammed colonies appeared at 15 days after transfection. After 20 days, individual iPS cell colonies were selected and subsequently passaged and maintained in hESF9 medium with TGF-β1 (2 ng/ml) (hESF9T) in dishes coated with fibronectin (Fig. 3-C). After 33 days in culture, ALP-positive colonies were counted; the efficiency of reprogramming was 0.23–0.39%. By contrast, iPS cell colonies did not emerge at all when cells were not re-plated on fibronectin after viral infection (data not shown). When TGF-β1 was present throughout the reprogramming procedure using hESF9T medium, the number of iPS colonies were 10-fold lower than that in